
ProSpec RL: Plan Ahead, then Execute.

Liangliang Liu¹, Yi Guan¹, BoRan Wang², Rujia Shen¹, Yi Lin¹, Chaoran Kong¹, Lian Yan¹,
Jingchi Jiang^{3*}

¹The Faculty of Computing, Harbin Institute of Technology, Harbin, China

²The Artificial Intelligence Institute, Harbin Institute of Technology, ShenZhen, China

³The Artificial Intelligence Institute, Harbin Institute of Technology, Harbin, China

{liull, shenrujia, linyi, kongchaoran, yanlian}@stu.hit.edu.cn

{guanyi, wangboran, jiangjingchi}@hit.edu.cn

Abstract

Imagining potential outcomes of actions before execution helps agents make more informed decisions, a prospective thinking ability fundamental to human cognition. However, mainstream model-free Reinforcement Learning (RL) methods lack the ability to proactively envision future scenarios, plan, and guide strategies. These methods typically rely on trial and error to adjust policy functions, aiming to maximize cumulative rewards or long-term value, even if such high-reward decisions place the environment in extremely dangerous states. To address this, we propose the Prospective (ProSpec) RL method, which makes higher-value, lower-risk optimal decisions by imagining future n-stream trajectories. Specifically, ProSpec employs a dynamic model to predict future states (termed “imagined states”) based on the current state and a series of sampled actions. Furthermore, we integrate the concept of Model Predictive Control and introduce a cycle consistency constraint that allows the agent to evaluate and select the optimal actions from these trajectories. Moreover, ProSpec employs cycle consistency to mitigate two fundamental issues in RL: augmenting state reversibility to avoid irreversible events (low risk) and augmenting actions to generate numerous virtual trajectories, thereby improving data efficiency. We validated the effectiveness of our method on the DMControl benchmarks, where our approach achieved significant performance improvements. Code will be open-sourced upon acceptance.

1 Introduction

Reinforcement Learning (RL) has proven indispensable for solving continuous decision problems [1, 2, 3]. Current RL research falls into two main categories: model-based and model-free methods. Model-based methods involve constructing a world model to simulate an interactive environment, which helps the agent predict future trajectories for optimal decision-making. However, these methods can be expensive and prone to failure due to discrepancies between the world model and reality [4]. On the other hand, model-free methods refine the policy function through trial-and-error learning, often outperforming model-based techniques in continuous control tasks [5]. However, these methods require frequent interaction with the environment, which is risky or costly in real-world applications [6], and suffer from low data efficiency when learning from complex, high-dimensional observations (such as image pixels) based on limited experience.

Training model-free methods using low data efficiency and sparse signals to fit high-performance feature encoders is challenging and prone to suboptimal convergence [7]. In contrast, humans can learn to play simple arcade games in minutes [8], while even state-of-the-art RL algorithms require billions of frames to reach human-level performance [9]. Moreover, collecting such large amounts of interaction data is impractical, especially in domains such as autonomous driving and robot control.

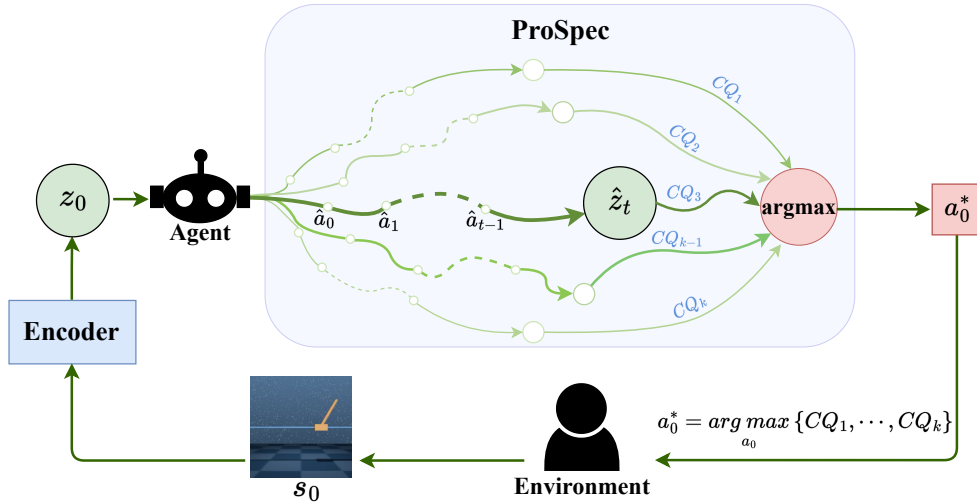


Figure 1: ProSpec RL process. First, the encoder encodes the initial state s_0 provided by the environment into a latent state representation z_0 . Upon receiving z_0 , the agent performs t step forward predictions from multiple perspectives (k) within ProSpec, resulting in k predicted future states $\{\hat{z}_{t1}, \dots, \hat{z}_{tk}\}$. Then ProSpec chooses the optimal action a_0^* to execute as $a_0^* = \arg \max_{a_0} \{CQ_1, \dots, CQ_k\}$, where $CQ_i = \sum_{j=0}^t \gamma^j Q(\hat{z}_j, \hat{a}_j)$ is the cumulative discounted return.

Currently, researchers are investigating data efficiency challenges from various angles. Including leveraging model-based world models to aid in policy learning [10, 11], employing data augmentation techniques to augment diversity in image appearances [12, 13], and introducing auxiliary tasks to assist in state representation learning [14, 15, 3, 16, 17], among other approaches. While many of these methods involve creating additional training processes to accelerate agent training, **the challenge of limited experience continues to impede the model’s exceptional performance.**

Learning planning is often deemed more critical than learning policies [5, 18, 19]. In cognitive neuroscience and psychology, planning is considered a facet of prospective thinking [20], which aids in predicting and adapting to future changes, envisioning potential problems or dangers, devising strategies to enhance problem-solving abilities, and setting future goals to drive action [21]. Ideally, prospective thinking is highly relevant to continuous decision-making tasks, where current actions can have irreversible consequences on future scenarios. However, current model-free methods lack planning capabilities, **thus relying solely on trial and error may lead to unacceptable risks.**

In this work, we introduce ProSpec, a model-free RL method that harnesses prospective thinking to envision potential future scenarios and make optimal decisions with higher value and lower risk through planning. More importantly, ProSpec could address data efficiency concerns by generating numerous virtual trajectories through imagination. Specifically, we model prospective thinking using a Flow-based Reversible Dynamics Model (FDM) and a Model Predictive Control (MPC)-based block. The FDM predicts prospective states in latent space in the forward process. In the backward process, we enforce cycle consistency constraints on the reversibility of prospective states to prevent the failure of prospective trajectories in irreparable states. Furthermore, we augment actions in a self-supervised learning fashion to generate numerous virtual trajectories and improve the efficiency of RL data. The MPC block employs the concept of MPC to facilitate exploratory interaction between the agent and the FDM, with the objective of exploring future scenarios from diverse perspectives. We summarize the contributions of this work as follows:

- We introduce a model-free method that integrates prospective thinking by incorporating a Flow-based Reversible Dynamics Model (FDM) for predicting prospective states, combined with cycle consistency to maintain state traceability. This enables the agent to explore future scenarios from various perspectives and identify optimal decisions with higher value and lower risk.

- Within our reversible framework, we introduce action augmentation in a self-supervised manner, generating multiple state-action trajectories to improve data efficiency.
- We validate the effectiveness of ProSpec through experiments on DeepMind benchmarks, showing significant performance improvements.

2 Related work

2.1 Prospective thinking

The capacity to anticipate the future represents as a crucial facet of human cognition, recently garnering substantial attention from researchers [20, 22, 23]. In psychology, prospective thinking is defined as the ability to mentally simulate the future, involving the extraction of information from episodic and semantic memory (such as detailed information about past states) as well as more abstract, schematic, and conceptual knowledge (such as envisioning general goals or events) [24, 25, 26]. Broadly, prospective thinking involves two main aspects: 1) predicting future scenarios and 2) guiding decisions for those scenarios. In deep learning, methods such as Model Predictive Control (MPC) and model-based Reinforcement Learning (RL) appear to encapsulate certain aspects of prospective thinking.

Model-based RL methods aim to construct an internal model, often referred to as a "World Model," to simulate the environment. This model helps predict future states and rewards, guiding the agent's decision-making and planning. Examples include PILCO [27], Dyna-Q [28], and World models [29]. On the other hand, MPC-based methods utilize the world model to optimize trajectories within a shorter time horizon. Examples of such methods include MuZero, Eff.Zero [30], and TD-MPC [5]. However, these approaches heavily rely on accurate environmental modeling and are limited by the complexity of state spaces. Consequently, model-based approaches often struggle to outperform simpler model-free methods in continuous control tasks [5]. Model-free methods, in contrast, learn policies through trial and error, directly interacting with the environment without the need for a World Model. This method is easy to implement and adapts well to complex environments. However, due to the frequent interaction with the environment and the lack of prediction of future states or consequences, it can lead to risky exploration of the environment [6].

Building upon this, we merge the planning capabilities of model-based methods to enhance model-free methods. To achieve this, we introduce a dynamics model into model-free methods, enabling the prediction of future scenarios. Additionally, we integrate the concept of MPC with value consistency to aid decision-making and guidance for future scenarios. Our objective is to leverage prospective thinking in selecting the optimal path while maintaining the trial-and-error learning approach of model-free methods. This integration aims to enhance the effectiveness of model-free methods in learning.

2.2 Data-Efficient Reinforcement Learning

When confronted with a limited amount of interaction data, the performance of both model-based and model-free methods experiences a significant decline. Researchers have extensively investigated this issue from various angles [3, 10, 11, 14, 15, 16, 17]. For example, SiMPLe utilizes collected data to learn a world model and generate imagined trajectories. They achieved outstanding results in multiple games under the setting of 100k frames, albeit at the cost of several weeks of training time. Subsequent studies, such as DataEfficient Rainbow [31] and OTRainbow [32], have demonstrated that merely increasing the number of steps in multi-step returns and conducting more frequent parameter updates can lead to improved performance under conditions of low data efficiency.

Consequently, there is growing interest in using computer vision techniques to enhance representation learning in RL [12, 13, 7]. For example, DrQ [7] and RAD [13] showed that moderate image augmentation can significantly improve the efficiency of RL data, outperforming previous methods using world models in model-based approaches. Yarats et al. [12] introduced image reconstruction as an auxiliary loss function in RL to improve data efficiency. Inspired by contrastive learning in representation learning, CURL [33] incorporated contrastive loss into RL, allowing the algorithm to distinguish representations of different states through contrastive loss and promote the generation of similar embeddings for similar states. In addition, some studies aim to incorporate dynamical models to help agents predict future events, thereby generating multiple virtual trajectories to improve

feature representation learning. For example, SPR [5], PBL [34], and SLAC [35], among others. Subsequently, EfficientZero [36] integrated SPR’s prediction loss into MuZero, improving the quality of internal state representations through self-generated predictions within the model.

Recently, researchers have incorporated cycle consistency into dynamics models [14, 17] to ensure that generated virtual trajectories maintain consistency and coherence with real-world behavior. The basic concept of cycle consistency involves performing a forward transformation from A to B using two transformation models, followed by a reverse transformation from A' back to B , and imposing consistency constraints between the original input A and the reconstructed input A' . For example, PlayVirtual [14] introduced backward dynamics models based on SPR, and established a loop through constraints between forward and backward dynamics models to improve feature representation learning via cycle consistency. VCR [17] introduced the concept of value consistency, where their dynamics model is constrained by Q-values computed with the real environment, enabling the model to learn representations directly related to decision-making, thereby improving model performance.

These successful cases demonstrate the effectiveness of cycle consistency in improving data efficiency. However, this approach often requires additional training to construct a backward dynamics model (as seen in PlayVirtual [14]), or directly imposing consistency constraints on learning from real environment policies. The latter approach may be susceptible to deviations in value functions caused by high-bias environments, as observed in VCR [17]. Therefore, in this study, we propose a novel approach that utilizes a simple flow-based dynamics model for both forward and backward predictions. In addition, cycle consistency is employed to improve data and state, ensuring the generation of numerous imagined trajectories under low-risk constraints to mitigate data efficiency issues.

3 Methods

In this section, we will systematically introduce the proposed ProSpec method. First, we will review some preliminary work. Then, we will present the overall framework of ProSpec.

3.1 Preliminaries: Reinforcement Learning

Reinforcement learning (RL) typically uses Markov decision processes (MDPs) to solve continuous decision problems, denoted as $\langle \mathcal{S}, \mathcal{A}, \mathcal{T}, \mathcal{R}, \gamma \rangle$. Here \mathcal{S} represents a finite set of states; \mathcal{A} is the action space; $\mathcal{T}(s_t, a_t, s_{t+1}) = P(s_{t+1}|s_t, a_t)$ is the dynamic function, which defines the probability of transition from state s_t to s_{t+1} after taking action a_t ; $\mathcal{R}(s_t, a_t)$ is the reward function, and $\gamma \in (0, 1]$ is the discount factor. The goal of RL is to enable the agent to learn how to maximize the expected discounted cumulative payoff $G_t = \sum_{\tau=0}^{\infty} \gamma^\tau \mathcal{R}(s_{t+\tau}, a_{t+\tau})$ by choosing actions at each time t . The agent’s decision process is guided by the policy $\pi(a_t|s_t)$, which maps the current state to the action selection. The action-value function $Q_\pi(s_t, a_t) = \mathbb{E}_\pi[G_t|s_t, a_t]$ evaluates the expected payoff of taking action a_t in state s_t and following policy π . This paper focuses on value-based RL methods, specifically Q-learning, which approximates the optimal policy π^* using the Bellman equation [37]. Therefore, Soft Actor-Critic (SAC) is employed as the policy algorithm, given that it is a widely utilized gradient-based algorithm for continuous control that incorporates policy entropy as an additional reward to encourage exploration. The overall training objective of SAC is as follows:

$$\mathcal{J}_\theta = \mathcal{L}_{\text{critic}} + \mathcal{L}_{\text{actor}} + \mathcal{L}_\alpha \tag{1}$$

where, $\mathcal{L}_{\text{critic}}$, $\mathcal{L}_{\text{actor}}$ and \mathcal{L}_α represent the critic loss, actor loss and temperature loss, respectively (see the supplementary material for details).

3.2 Overall Framework

In this paper, we introduce the ProSpec method, which aims to incorporate prospective thinking into model-free methods. ProSpec consists of two main components: first, the Flow-based Dynamics Model for predicting future scenarios, and second, the prospective unit that integrates Model Predictive Control and value consistency to guide decision-making. Figure 1 shows the process of ProSpec RL. In the following sections, we provide detailed explanations of each component.

Flow-based Dynamics Model (FDM). The FDM predicts the future and retroactively infers previous latent states, crucial in ProSpec. Unlike PlayVirtual [14], which employs separate models for these

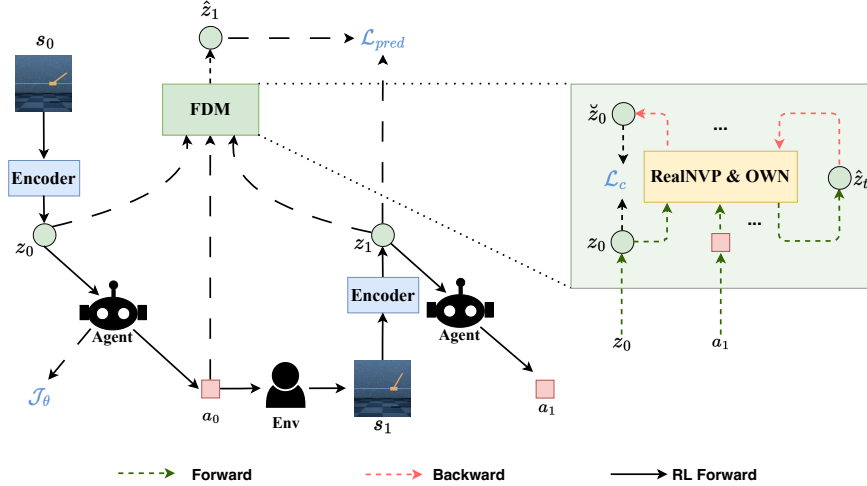


Figure 2: Training Procedure of ProSpec. Here, \mathcal{J}_θ represents the reinforcement learning loss; \mathcal{L}_{pred} denotes the prediction loss of the Flow-based Dynamics Model (FDM); \mathcal{L}_c stands for the cycle consistency loss.

tasks, our approach employs a single model for both, avoiding training instability. We utilize Real-valued non-volume preserving (RealNVP) [38], a flow-based neural network that performs bijective coupling transformations. RealNVP operates via bijective coupling layers, with each layer handling parts of the input $a_t \in \mathbb{R}^{1:d}$ and $z_t \in \mathbb{R}^{d+1:D}$ separately. It applies transformations using affine functions for scaling $\exp(sc_i(\cdot))$ and translation $t_i(\cdot)$, along with element-wise multiplication ‘ \odot ’ and addition ‘+’ operations. This enables the computation of the forward process as:

$$\begin{aligned} \hat{z}_{t+1}^{1:d} &= a_t \odot \exp(sc_2(z_t)) + t_2(z_t) \\ \hat{z}_{t+1}^{d+1:D} &= z_t \odot \exp(sc_1(a_t)) + t_1(a_t) \end{aligned} \quad (2)$$

and the backward processes can be calculated as:

$$\begin{aligned} z_t &= (\hat{z}_{t+1}^{d+1:D} - t_1(\hat{z}_{t+1}^{1:d})) \odot \exp(-sc_1(\hat{z}_{t+1}^{1:d})) \\ a_t &= (\hat{z}_{t+1}^{1:d} - t_2(\hat{z}_{t+1}^{d+1:D})) \odot \exp(-sc_2(\hat{z}_{t+1}^{d+1:D})) \end{aligned} \quad (3)$$

Note that there exists a dimensional inconsistency between $\hat{z}_{t+1} \in \mathbb{R}^D$ and $z_t \in \mathbb{R}^{d+1:D}$. Typically, a feed-forward neural network, represented as $f(z_t; \theta)$ with parameters θ , endeavors to fit training data and predict the subsequent latent state \hat{z}_{t+1} . The network’s transformation can be expressed as $\hat{z}_{t+1} = W \cdot z_t + B$, where $W \in \mathbb{R}^{n \times n}$ and $B \in \mathbb{R}^{n \times n}$ denote the weights and biases, collectively denoted as $\theta = \{W, B\}$. However, owing to the typical non-invertibility of W , conducting backward inference (i.e., directly computing $z_t = W^{-1}(\hat{z}_{t+1} - B)$) poses challenges. To ensure reversibility, Orthogonal Weight Normalization (OWN) [39] is employed, supporting straightforward backward inference by enforcing orthogonality in the weights, unlike the structural design in invertible networks. Consequently, the backward process can be reformulated as:

$$z_t = W^T(\hat{z}_{t+1} - B), \quad W \in \mathcal{O}^{n \times n} \quad (4)$$

where the matrix family $\mathcal{O}^{n \times n} = \{W \in \mathbb{R}^{n \times n} \mid WW^T = W^{-1}W = I\}$ (see [39] for more details). By using the combination of RealNVP and OWN, we can effectively achieve bidirectional transformation between z_t and \hat{z}_{t+1} .

Forward States Prediction with FDM. In the MDP framework, a one-step transition (s_t, a_t, s_{t+1}) describes the process of transitioning from the current state $s_t \in \mathcal{S}$ to the next state s_{t+1} by taking action $a_t \in \mathcal{A}$. Considering the crucial aspect of prospective thinking, i.e., the ability to predict future scenarios, is very important for RL tasks. Many studies focus on training dynamic models to predict future states to learn good feature representations [16, 34, 35]. In this study, the FDM $h(\cdot, \cdot)$ is used to simulate the dynamics function \mathcal{T} in the latent embedding space, allowing us to explore the future from multiple perspectives. As shown in Figure 2, the encoder $f(\cdot, \cdot)$ first converts the image-based

observation/state s_0 into a latent representation $z_0 = f(s_0)$. Then, based on the sampled action set $\hat{A}(z_0) = \{\hat{a}_0, \dots, \hat{a}_k\}$ from k perspectives, the FDM predicts the latent state set $\hat{Z}_{0:t}$ for t future steps. Formally:

$$\begin{aligned} \hat{z}_0 &= z_0 = f(s_0) \\ \hat{z}_t &= h(\hat{a}_{t-1}, \hat{z}_{t-1}) \\ \hat{Z}_{0:t} &= \{h(\hat{A}_0(z_0), z_0), \dots, h(\hat{A}_t(\hat{z}_t), \hat{z}_t)\} \end{aligned} \quad (5)$$

The optimization objective of the FDM $h(\cdot, \cdot)$ is to minimize the difference (error) between the predicted latent state sequence \hat{z}_t and the latent feature sequence z_t directly extracted from the original observation/state, where $z_t = f_T(s_t)$. Following SPR [16], we use ‘‘projection’’ and cosine similarity on DMControl to predict the error, aiming to achieve the following objective:

$$\mathcal{L}_{\text{pred}} = - \sum_{k=1}^K \left(\frac{\hat{z}_{t+k}}{\|\hat{z}_{t+k}\|_2} \right)^\top \left(\frac{z_{t+k}}{\|z_{t+k}\|_2} \right) \quad (6)$$

Where z_t is referred to as the target embedding, generated by the stop-gradient version of the online encoder $f(\cdot)$ termed as the target encoder $f_T(\cdot)$.

Backward Return to Previous States with FDM. The backward process of the FDM aims to derive the previous latent states \check{z}_t based on the given subsequent latent state \check{z}_{t+1} and the causal action \hat{a}_t . We enforce constraints on the trajectories generated by FDM, ensuring cycle consistency to prevent forward trajectories from encountering irreparable states. Given \hat{a}_t and \check{z}_{t+1} , the reversibility of FDM allows us to easily trace back to the previous latent dynamics \check{z}_t . Formally, given the hidden state \check{z}_{t+K} and a sequence of actions $\hat{a}_{t+K-1:t} = \{\hat{a}_{t+K-1}, \dots, \hat{a}_t\}$, we iteratively compute the previous K state sequence $\check{z}_{t+k-1:t} = \{\check{z}_{t+k-1}, \dots, \check{z}_t\}$ using the inverse function $h^{-1}(\cdot, \cdot)$:

$$\check{z}_{t+k-1} = \begin{cases} h^{-1}(\hat{a}_{t+k-1}, \check{z}_{t+k}), & \text{if } k = K \\ h^{-1}(\hat{a}_{t+k-1}, \check{z}_{t+k}), & \text{if } k = K - 1, \dots, 1. \end{cases} \quad (7)$$

Using FDM, we can easily generate both a forward and a backward trajectory given the current state and a sequence of actions, forming a cycle forward-inverse trajectory. Ideally, the initial latent state z_t of this cycle trajectory should coincide with the final latent state \check{z}_t . Therefore, as shown in the right side of Figure 2, we introduce cycle consistency constraints between the initial state z_0 and the final state \check{z}_0 to prevent prospective trajectories from entering irreparable states. In addition, we improve actions in an unsupervised manner by generating or sampling virtual actions to create diverse virtual trajectories, which promotes data efficiency without relying solely on real trajectories for supervised learning. The inclusion of cycle consistency constraints serves a dual purpose, enhancing both the learning of feature representations and the reversibility of states to preclude irreversible events, while also elevating the training efficiency of the weight matrix W in OWN.

The optimization objective of cycle consistency is to minimize the spatial distance $d(z_t, \check{z}_t)$ between two latent states z_t and \check{z}_t . Given the latent state representation z_t at time t , we randomly sample M actions from the action space \mathcal{A} . Therefore, the loss function for cycle consistency is defined as:

$$\mathcal{L}_c = \frac{1}{M} \sum_{m=1}^M d(z_t, \check{z}_t) \quad (8)$$

Guiding Future Scenario Decisions with Model Predictive Control. In RL, policies π are formed by neural networks to approximate the optimal policy $\pi_\theta(\cdot|s_t)$. In classical control tasks, however, π takes the form of trajectory optimization, often seeking a local best solution at each time step [5]. This involves predicting the best actions $a_{t:t+H}$ over a short horizon H and executing the first action a_t , a method known as MPC:

$$\pi_\theta^{\text{MPC}} = \arg \max_{a_{t:t+H}} \mathbb{E} \left[\sum_{j=t}^H \gamma^j \mathcal{R}(s_j, a_j) \right] \quad (9)$$

In the SAC framework, the actor selects samples from the distribution of state-action pairs (s_t, a_t) according to the current policy π : $a_t \sim \pi_\theta(\cdot, s_t)$. To incorporate prospective thinking into model-free methods, we introduce the concept of MPC. Specifically, a_t is chosen as the first action that maximizes the long-term reward within a finite range H from $j \in [1, n]$:

$$a_t = \arg \max_{a_{t:t+H}} \sum_{j=t}^H \gamma^j \mathcal{R}(s_j, a_j) \quad (10)$$

Due to its deep understanding of the environment model, MPC autonomously computes rewards from simulated trajectories (i.e., state-action pairs), which is distinct from model-free methods where the reward function $\mathcal{R}(\cdot, \cdot)$ is provided by the environment, not computed by itself. Furthermore, it’s essential to distinguish this approach from the iterative Q-value estimation in reinforcement learning, which prioritizes short-term gains over long-term cumulative rewards.

Therefore, we introduce the value consistency to guide the prospective action selection process. The evaluation of actions through prospective thinking should ideally be consistent with the Q-values determined by the RL policy π , ensuring the agent selects actions that provide the maximum long-term benefit in each state. As shown in Figure 1, we construct an action set $\hat{A}(z_0) = \{\hat{a}_0, \dots, \hat{a}_t\}$ from the current latent state z_0 , which includes t potential actions. For each pair of trajectories $(\hat{z}_i, a_i \in \hat{A}(s_t))$, we use $Q(\hat{z}_i, \hat{a}_i)$ as a proxy for the reward function $\mathcal{R}(\cdot, \cdot)$, where $i \in [1, t]$. Subsequently, after computing the cumulative discounted rewards $CQ_i = \sum_{j=0}^t \gamma^j Q(\hat{z}_j, \hat{a}_j)$ for each trajectory set, we determine the locally optimal action $a_0^* = \arg \max_{a_0} \{CQ_1, \dots, CQ_k\}$. Ensuring the consistency of Q-values guarantees that the selected action a_t^* at each time step is the optimal choice according to the current policy, thus fulfilling the function of decision-making and guiding future scenarios.

Overall Objective. As shown in Figure 2, the overall training objective of our approach can be summarized as follows:

$$\mathcal{L}_{total}(\theta) = \underbrace{\mathcal{J}_\theta}_{\text{RL}} + \underbrace{\lambda_{pred} \mathcal{L}_{pred}(\theta)}_{\text{pred}} + \underbrace{\lambda_c \mathcal{L}_c(\theta)}_{\text{Cycle Consistency}} \quad (11)$$

where θ represents all model parameters used to compute the above loss functions, \mathcal{J}_θ is the loss function for RL (see section 1), and λ_{pred} and λ_c are hyperparameters that weight different losses (more detailed can be seen in the supplementary material).

4 Experiments

In this section, we will provide a detailed introduction to the evaluation environment used in this paper, including experimental settings, experimental details, and evaluation metrics. Then, we perform a series of ablation experiments to analyze the key components of our method.

4.1 Setup for Evaluation

Environments. We conducted benchmark tests on ProSpec in environments with limited interaction, using the DeepMind Control Suite (DMControl) for continuous control testing [40]. Following the practices of most researchers [7, 12, 14, 31, 41, 42, 43], we evaluated the performance after training for 100k and 500k interaction steps in the DMControl environment, selecting a total of 6 games for performance evaluation.

Baseline. In this work, we consider SPR [16] as a strong baseline. We also selected Dreamer [44], SAC+AE [7], SLAC [34], CURL [33], DrQ [12], SPR [16], PlayVirtual [14], and VCR [17] as baselines. It is worth noting that since SPR was originally designed for offline tasks, we adapted SPR for continuous tasks using a SAC-based approach (SPR[†]).

Implementation Details. We used the encoder and policy network architecture of CURL [33] as the basic network. The contrastive loss component was removed from CURL, and we introduced BYOL [45], creating a baseline solution similar to SPR. To generate imaginary trajectories in this environment, the prediction horizon was set to 6, and action generation was achieved by randomly sampling from a uniform distribution over the continuous action space. Additional implementation details are provided in the Appendix.

Evaluation Metrics. In DMControl, the maximum achievable score for each environment is capped at 1000 [40]. Consistent with previous studies [7, 33, 34, 46, 44], we evaluated model performance across six common environments and used the median score to represent overall performance. To reduce potential variance in benchmarking results, we performed ProSpec evaluations on DMControl using 10 random seeds for each game. For the 100k step, we reran the official code for SPR and PlayVirtual with 10 random seeds and recorded the final results. We did not rerun the code for VCR as we were unable to obtain the official implementation. Due to limited computational resources, we report the 500k results directly from the respective papers. The entire implementation was using PyTorch [47], with network training performed on an NVIDIA RTX 3090 GPU.

Table 1: Scores obtained by different methods on DMControl-100k and DMControl-500k (mean and standard deviation). ProSpec was run with 10 random seeds, and the overall median scores were recorded for evaluation comparison. The results for VCR are reproduced from the original paper because we do not have access to the official VCR code.

100k Step Scores	Dreamer	SAC+AE	SLAC	CURL	DrQ	SPR [†]	PlayVirtual	ProSpec	VCR
Finger, spin	341±70	740±64	693±141	767±56	901±104	835±154	866 ±103	875±104	795±157
Cartpole, swingup	326±27	311±11	-	582±146	759±92	806±45	824±57	833±34	815±47
Reacher, easy	314±155	274±14	-	538±33	601±213	667±173	685±216	782±137	763±112
Cheetah, run	235±137	267±24	319±56	299±48	344±67	434±48	466±67	477±24	422±54
Walker, walk	277±12	394±22	361±73	403±24	612±164	398±145	596±184	507±60	650±143
Ball in cup, catch	246±174	391±82	512±110	769±43	913±53	814±263	921±31	927±17	858±85
Median Score	295.5	351	436.5	560	685.5	736.5	745.5	807.5	779
Finger, spin	796±183	884±128	673±92	926±45	938±103	924±132	963±40	973±14	972±25
Cartpole, swingup	762±27	735±63	-	841±45	868±10	870±12	865±11	871±13	854±26
Reacher, easy	793±164	627±58	-	929±44	942±71	925±79	942±66	965±14	938±37
Cheetah, run	570±253	550±34	640±19	518±28	660±96	716±47	716±47	719±51	661±32
Walker, walk	897±49	847±48	842±51	902±43	921±45	916±75	928±30	954±19	930±18
Ball in cup, catch	879±87	794±58	852±71	959±27	963±9	963±8	967±5	972±5	958±4
Median Score	794.5	764.5	757.5	914	929.5	920	935	959.5	934

4.2 Performance Comparison with State-of-the-Arts

As shown in Table 1, our method surpassed the performance of most other methods by achieving five of the top scores in six environments, regardless of the limited 100k or 500k interactions. Furthermore, when considering the median scores, our method achieved the highest rankings in the following two aspects: (i) In the DMControl-100k environment with limited interaction data, our method achieves the highest median score of 807.5. This outperforms PlayVirtual by 8.32%, VCR by 3.66%, SPR by 9.64%, DrQ by 17.80%, and CURL by 44.20%. (ii) Our method achieves a median score of 959.5 and comes close to the maximum score of 1000 in four environments. These results demonstrate the exceptional performance of our method even with limited data. Furthermore, our method shows a significant improvement in performance across different environments.

4.3 Analysis

In this section, we performed an ablation study in the DMControl-100k to analyze the key components of ProSpec. Due to limited computing resources, we experimented using 5 random seeds.

Effectiveness of FDM and Prospective Thinking. To explore the effect of prospective thinking on RL tasks, we evaluated ProSpec without prospective thinking (ProSpec-NP) and compared it to SPR[†] and PlayVirtual. The results are detailed in Table 2. As can be seen: (i) ProSpec improved by 55.5 scores over ProSpec-NP; (ii) ProSpec-NP outperformed PlayVirtual by 6.5 scores; (iii) ProSpec increased PlayVirtual’s median score from 752.0 to 807.5. Several factors may explain these results: First, using human-like prospective thinking, ProSpec explores the future from multiple perspectives and selects higher-value, lower-risk decisions, improving its performance by 55.5 scores over ProSpec-NP. Typically, Prospective thinking resembles residual structures in neural networks, allowing the model to approach local optima with each decision, leading to consistent performance improvements. Second, the flow-based dynamics model provides more accurate backward predictions, while cycle consistency augments state traceability and guides low-risk decisions, improving ProSpec’s performance over PlayVirtual. Finally, self-supervised methods generate multiple state-action trajectories, increasing data efficiency and allowing ProSpec to outperform SPR[†].

The Impact of Cycle Consistency on ProSpec. As described in Section 3.2, cycle consistency is used to address two fundamental issues in RL: augmenting state traceability to avoid irretrievable events (low risk), and generating a large number of virtual trajectories to improve data efficiency with augmented actions. We evaluated the performance of ProSpec without cycle consistency constraints (referred to as ProSpec-NC) and compared it to SPR methods. As shown in Table 3, regularizing the encoder with \mathcal{L}_c in ProSpec-NC resulted

Table 2: Effectiveness of FDM and Prospective Thinking.

	Median Score
SPR[†]	736.5
PlayVirtual	745.5
ProSpec-NP	752.0
ProSpec	807.5

Table 3: The impact of cycle consistency on ProSpec.

	Median Score
SPR[†]	736.5
ProSpec-NC	752.8
ProSpec	807.5

in a gain of 2.21%, while regularizing both the encoder and the FDM resulted in a gain of 7.27%. It is clear that cycle consistency can benefit the training of the FDM, but the greater benefit comes from the learning of the feature representations in the encoder [14].

Impact of Perspective Count k . We explored how the number of perspectives k affects ProSpec in lookahead tasks. Experiments were performed with different perspectives $k \in [1, 9]$, and we recorded the median results under different prediction steps $t \in [1, 15]$ (additional results are available in the supplementary material). Table 4 presents these results: (i) at $k = 3$, ProSpec achieved peak performance, marking an improvement of 6.85% over $k = 1$ and 1.9% over $k = 9$; (ii) contrary to expectations, the performance improvement does not scale linearly with the number of perspectives. While $k \geq 3$, the performance improvement reaches saturation and shows less differences. This may be because the actions sampled by the agent yield similar long-term rewards as the number of perspectives increases, resulting in insignificant differences in model performance.

Impact of Prediction Steps t on ProSpec. We examined the effect of prediction steps t on ProSpec’s performance, as shown in table 5. Similar to the previous experiment, we evaluated the median performance across different perspectives k . Our results can be summarized as follows: (i) Except for the finger-spin environments, ProSpec shows significant performance improvements in most environments. This suggests that ProSpec’s prospective thinking effectively uses future information to improve the effectiveness of current decisions, and improves model performance across different scenarios. (ii) ProSpec achieves optimal performance at $t = 6$, showing improvements of 6.25% and 6.18% over $t = 1$ and $t = 15$, respectively. (iii) Notably, ProSpec’s performance does not exhibit a linear increase with prediction steps t . Instead, beyond a certain threshold of t , performance growth begins to slow or even decline. This phenomenon may be due to the increased complexity of future states that the model attempts to capture with an excessive number of prediction steps, leading to additional prediction errors and compromising prediction accuracy.

Table 4: Impact of perspective count k .

	k=1	k=3	k=6	k=9
Finger, spin	880.0	867.9	871.2	811.7
Cartpole, swingup	816.0	831.5	820.0	800.0
Reacher, easy	675.8	762.6	770.3	763.6
Cheetah, run	349.8	388.2	384.5	419.7
Walker, walk	424.6	561.4	517.6	516.5
Ball in cup, catch	845.1	905.5	905.8	934.4
Median Score	745.9	797.0	795.1	781.8

Table 5: Impact of prediction steps t on ProSpec.

	t=1	t=3	t=6	t=9	t=12	t=15
Finger, spin	877.6	813.0	820.6	785.3	772.3	810.4
Cartpole, swingup	813.0	793.0	818.0	817.0	829.0	836.0
Reacher, easy	695.8	670.4	785.2	675.3	766.7	699.5
Cheetah, run	361.7	375.3	466.5	415.3	368.6	382.9
Walker, walk	522.8	573.7	581.4	555.4	522.4	539.0
Ball in cup, catch	868.7	908.1	927.2	926.5	921.8	918.0
Median Score	754.4	726.6	809.0	731.4	771.3	774.9

5 Conclusion and Limitation

To imbue deep RL with cognitive abilities akin to those of humans—namely, prospective thinking—we propose a novel method named ProSpec. ProSpec employs a reversible flow-based dynamics model to predict latent future outcomes, drawing on the concept of Model Predictive Control to guide decision-making in anticipation of future scenarios. This approach enables RL to simulate future n-stream trajectories, facilitating high-value, low-risk optimal decision-making. Additionally, ProSpec augments state traceability through cycle consistency, reducing environmental risks and leveraging this to augment actions, thus generating a wealth of virtual trajectories to improve data efficiency. We conducted a large number of experiments at DMControl and the results confirmed the effectiveness of ProSpec. However, due to the necessity of exploring future scenarios from multiple perspectives, our method incurs additional overhead in training the agent. In addition, ProSpec is currently tailored for value-based RL methods; future research endeavors will aim to discover a universally applicable RL approach that incorporates prospective thinking.

References

- [1] Volodymyr Mnih, Koray Kavukcuoglu, David Silver, Andrei A Rusu, Joel Veness, Marc G Bellemare, Alex Graves, Martin Riedmiller, Andreas K Fidjeland, Georg Ostrovski, et al. Human-level control through deep reinforcement learning. *nature*, 518(7540):529–533, 2015.
- [2] David Silver, Julian Schrittwieser, Karen Simonyan, Ioannis Antonoglou, Aja Huang, Arthur Guez, Thomas Hubert, Lucas Baker, Matthew Lai, Adrian Bolton, et al. Mastering the game of go without human knowledge. *nature*, 550(7676):354–359, 2017.
- [3] Julian Schrittwieser, Ioannis Antonoglou, Thomas Hubert, Karen Simonyan, Laurent Sifre, Simon Schmitt, Arthur Guez, Edward Lockhart, Demis Hassabis, Thore Graepel, et al. Mastering atari, go, chess and shogi by planning with a learned model. *Nature*, 588(7839):604–609, 2020.
- [4] YANG Zhihe and Yunjian Xu. Dmbp: Diffusion model based predictor for robust offline reinforcement learning against state observation perturbations. In *The Twelfth International Conference on Learning Representations*, 2023.
- [5] Nicklas Hansen, Xiaolong Wang, and Hao Su. Temporal difference learning for model predictive control. *arXiv preprint arXiv:2203.04955*, 2022.
- [6] Sergey Levine, Aviral Kumar, George Tucker, and Justin Fu. Offline reinforcement learning: Tutorial, review, and perspectives on open problems. *arXiv preprint arXiv:2005.01643*, 2020.
- [7] Denis Yarats, Amy Zhang, Ilya Kostrikov, Brandon Amos, Joelle Pineau, and Rob Fergus. Improving sample efficiency in model-free reinforcement learning from images. In *Proceedings of the AAAI Conference on Artificial Intelligence*, volume 35, pages 10674–10681, 2021.
- [8] Marc G Bellemare, Yavar Naddaf, Joel Veness, and Michael Bowling. The arcade learning environment: An evaluation platform for general agents. *Journal of Artificial Intelligence Research*, 47:253–279, 2013.
- [9] Adrià Puigdomènech Badia, Bilal Piot, Steven Kapturowski, Pablo Sprechmann, Alex Vitvitskyi, Zhaohan Daniel Guo, and Charles Blundell. Agent57: Outperforming the atari human benchmark. In *International conference on machine learning*, pages 507–517. PMLR, 2020.
- [10] Huining Yuan, Hongkun Dou, Xingyu Jiang, and Yue Deng. Task-aware world model learning with meta weighting via bi-level optimization. *Advances in Neural Information Processing Systems*, 36, 2024.
- [11] Chuning Zhu, Max Simchowitz, Siri Gadipudi, and Abhishek Gupta. Repo: Resilient model-based reinforcement learning by regularizing posterior predictability. *Advances in Neural Information Processing Systems*, 36, 2024.
- [12] Denis Yarats, Ilya Kostrikov, and Rob Fergus. Image augmentation is all you need: Regularizing deep reinforcement learning from pixels. In *International conference on learning representations*, 2020.
- [13] Misha Laskin, Kimin Lee, Adam Stooke, Lerrel Pinto, Pieter Abbeel, and Aravind Srinivas. Reinforcement learning with augmented data. *Advances in neural information processing systems*, 33:19884–19895, 2020.
- [14] Tao Yu, Cuiling Lan, Wenjun Zeng, Mingxiao Feng, Zhizheng Zhang, and Zhibo Chen. Playvirtual: Augmenting cycle-consistent virtual trajectories for reinforcement learning. *Advances in Neural Information Processing Systems*, 34:5276–5289, 2021.
- [15] Max Jaderberg, Volodymyr Mnih, Wojciech Marian Czarnecki, Tom Schaul, Joel Z Leibo, David Silver, and Koray Kavukcuoglu. Reinforcement learning with unsupervised auxiliary tasks. *arXiv preprint arXiv:1611.05397*, 2016.
- [16] Max Schwarzer, Ankesh Anand, Rishab Goel, R Devon Hjelm, Aaron Courville, and Philip Bachman. Data-efficient reinforcement learning with self-predictive representations. *arXiv preprint arXiv:2007.05929*, 2020.
- [17] Yang Yue, Bingyi Kang, Zhongwen Xu, Gao Huang, and Shuicheng Yan. Value-consistent representation learning for data-efficient reinforcement learning. In *Proceedings of the AAAI Conference on Artificial Intelligence*, volume 37, pages 11069–11077, 2023.
- [18] Michael Janner, Justin Fu, Marvin Zhang, and Sergey Levine. When to trust your model: Model-based policy optimization. *Advances in neural information processing systems*, 32, 2019.

- [19] Kendall Lowrey, Aravind Rajeswaran, Sham Kakade, Emanuel Todorov, and Igor Mordatch. Plan online, learn offline: Efficient learning and exploration via model-based control. *arXiv preprint arXiv:1811.01848*, 2018.
- [20] Daniel L Schacter, Donna Rose Addis, Demis Hassabis, Victoria C Martin, R Nathan Spreng, and Karl K Szpunar. The future of memory: remembering, imagining, and the brain. *Neuron*, 76(4):677–694, 2012.
- [21] Lisa G Aspinwall. The psychology of future-oriented thinking: From achievement to proactive coping, adaptation, and aging. *Motivation and emotion*, 29:203–235, 2005.
- [22] Peter McKiernan. Prospective thinking; scenario planning meets neuroscience. *Technological Forecasting and Social Change*, 124:66–76, 2017.
- [23] Lia Kvavilashvili and Jan Rummel. On the nature of everyday prospection: A review and theoretical integration of research on mind-wandering, future thinking, and prospective memory. *Review of General Psychology*, 24(3):210–237, 2020.
- [24] Daniel L Schacter and Donna Rose Addis. The cognitive neuroscience of constructive memory: remembering the past and imagining the future. *Philosophical Transactions of the Royal Society B: Biological Sciences*, 362(1481):773–786, 2007.
- [25] Demis Hassabis and Eleanor A Maguire. Deconstructing episodic memory with construction. *Trends in cognitive sciences*, 11(7):299–306, 2007.
- [26] Thomas Suddendorf and Michael C Corballis. The evolution of foresight: What is mental time travel, and is it unique to humans? *Behavioral and brain sciences*, 30(3):299–313, 2007.
- [27] Marc Deisenroth and Carl E Rasmussen. Pilco: A model-based and data-efficient approach to policy search. In *Proceedings of the 28th International Conference on machine learning (ICML-11)*, pages 465–472, 2011.
- [28] Baolin Peng, Xiujun Li, Jianfeng Gao, Jingjing Liu, Kam-Fai Wong, and Shang-Yu Su. Deep dyna-q: Integrating planning for task-completion dialogue policy learning. *arXiv preprint arXiv:1801.06176*, 2018.
- [29] David Ha and Jürgen Schmidhuber. World models. *arXiv preprint arXiv:1803.10122*, 2018.
- [30] Tianhe Yu, Garrett Thomas, Lantao Yu, Stefano Ermon, James Y Zou, Sergey Levine, Chelsea Finn, and Tengyu Ma. Mopo: Model-based offline policy optimization. *Advances in Neural Information Processing Systems*, 33:14129–14142, 2020.
- [31] Hado P Van Hasselt, Matteo Hessel, and John Aslanides. When to use parametric models in reinforcement learning? *Advances in Neural Information Processing Systems*, 32, 2019.
- [32] Kacper Piotr Kielak. Do recent advancements in model-based deep reinforcement learning really improve data efficiency? 2019.
- [33] Michael Laskin, Aravind Srinivas, and Pieter Abbeel. Curl: Contrastive unsupervised representations for reinforcement learning. In *International conference on machine learning*, pages 5639–5650. PMLR, 2020.
- [34] Zhaohan Daniel Guo, Bernardo Avila Pires, Bilal Piot, Jean-Bastien Grill, Florent Alché, Rémi Munos, and Mohammad Gheshlaghi Azar. Bootstrap latent-predictive representations for multitask reinforcement learning. In *International Conference on Machine Learning*, pages 3875–3886. PMLR, 2020.
- [35] Alex X Lee, Anusha Nagabandi, Pieter Abbeel, and Sergey Levine. Stochastic latent actor-critic: Deep reinforcement learning with a latent variable model. *Advances in Neural Information Processing Systems*, 33:741–752, 2020.
- [36] Danijar Hafner, Timothy Lillicrap, Mohammad Norouzi, and Jimmy Ba. Mastering atari with discrete world models. *arXiv preprint arXiv:2010.02193*, 2020.
- [37] Richard S Sutton and Andrew G Barto. *Reinforcement learning: An introduction*. MIT press, 2018.
- [38] Laurent Dinh, Jascha Sohl-Dickstein, and Samy Bengio. Density estimation using real nvp. *arXiv preprint arXiv:1605.08803*, 2016.

- [39] Lei Huang, Xianglong Liu, Bo Lang, Adams Yu, Yongliang Wang, and Bo Li. Orthogonal weight normalization: Solution to optimization over multiple dependent stiefel manifolds in deep neural networks. In *Proceedings of the AAAI Conference on Artificial Intelligence*, volume 32, 2018.
- [40] Yuval Tassa, Yotam Doron, Alistair Muldal, Tom Erez, Yazhe Li, Diego de Las Casas, David Budden, Abbas Abdolmaleki, Josh Merel, Andrew Lefrancq, et al. Deepmind control suite. *arXiv preprint arXiv:1801.00690*, 2018.
- [41] Ashley D Edwards, Laura Downs, and James C Davidson. Forward-backward reinforcement learning. *arXiv preprint arXiv:1803.10227*, 2018.
- [42] Oriol Vinyals, Igor Babuschkin, Wojciech M Czarnecki, Michaël Mathieu, Andrew Dudzik, Junyoung Chung, David H Choi, Richard Powell, Timo Ewalds, Petko Georgiev, et al. Grandmaster level in starcraft ii using multi-agent reinforcement learning. *Nature*, 575(7782):350–354, 2019.
- [43] Ziyu Wang, Tom Schaul, Matteo Hessel, Hado Hasselt, Marc Lanctot, and Nando Freitas. Dueling network architectures for deep reinforcement learning. In *International conference on machine learning*, pages 1995–2003. PMLR, 2016.
- [44] Danijar Hafner, Timothy Lillicrap, Jimmy Ba, and Mohammad Norouzi. Dream to control: Learning behaviors by latent imagination. *arXiv preprint arXiv:1912.01603*, 2019.
- [45] Jean-Bastien Grill, Florian Strub, Florent Altché, Corentin Tallec, Pierre Richemond, Elena Buchatskaya, Carl Doersch, Bernardo Avila Pires, Zhaohan Guo, Mohammad Gheshlaghi Azar, et al. Bootstrap your own latent—a new approach to self-supervised learning. *Advances in neural information processing systems*, 33:21271–21284, 2020.
- [46] Danijar Hafner, Timothy Lillicrap, Ian Fischer, Ruben Villegas, David Ha, Honglak Lee, and James Davidson. Learning latent dynamics for planning from pixels. In *International conference on machine learning*, pages 2555–2565. PMLR, 2019.
- [47] Adam Paszke, Sam Gross, Francisco Massa, Adam Lerer, James Bradbury, Gregory Chanan, Trevor Killeen, Zeming Lin, Natalia Gimelshein, Luca Antiga, et al. Pytorch: An imperative style, high-performance deep learning library. *Advances in neural information processing systems*, 32, 2019.